

Article

Soil Water Content and Temperature Dynamics under Grassland Degradation: A Multi-Depth Continuous Measurement from the Agricultural Pastoral Ecotone in Northwest China

Wenjing Yang ¹, Yibo Wang ^{1,2,*}, Chansheng He ^{1,3,*}, Xingyan Tan ¹ and Zhibo Han ¹

¹ College of Earth and Environmental Sciences, Lanzhou University, Lanzhou 730000, China

² State Key Laboratory of Frozen Soil Engineering, Northwest Institute of Eco-Environment and Resources, Chinese Academy of Sciences (CAS), Lanzhou 730000, China

³ Department of Geography, Western Michigan University, Kalamazoo, MI 49008, USA

* Correspondence: wangyib@lzu.edu.cn (Y.W.); he@wmich.edu (C.H.); Tel.: +86-136-5948-6653 (Y.W.)

Received: 22 June 2019; Accepted: 29 July 2019; Published: 2 August 2019



Abstract: The agricultural pastoral ecotone (APE) in Northwest China is an ecological transition zone in the arid area with a very fragile ecosystem. In recent years, the ecosystem has deteriorated sharply, and increasing desertification has made the regional ecosystem more vulnerable and sensitive. In this study, we analyzed (using classical statistical methods) spatial and temporal variations in soil water content (SWC) from 14 September 2016 to 22 April 2019 for high and low vegetation in two grassland sites in Yanchi County, Ningxia. The results showed that the largest average seasonal SWC occurred in autumn. The SWC of the first three layers (0 ÷ 15 cm) of the soil profile responded strongly to precipitation, whereas the SWC in deeper soil (30 ÷ 50 cm) could only be recharged markedly after continuous precipitation. Additionally, the growing process of plants proved to be a cause of variability in soil moisture profiles. Vegetation degradation sped up the course of desertification and decreased soil organic carbon content. These changes left the soil increasingly desiccated and enhanced soil variability. Meanwhile, vegetation degradation also prompted changes in soil temperature and shortened the soil's frozen time in winter. With the acceleration of global warming, if the process of vegetation degeneration continues and soil temperatures keep rising, the ecosystem is likely to undergo irreversible degradation.

Keywords: soil moisture; spatiotemporal variation; soil properties; precipitation

1. Introduction

The soil water content (SWC) is usually defined as water stored in unsaturated soil layers [1,2]. It plays an important role in the global water cycle by controlling the distribution of evaporation and infiltration [3]. It is also a critical link between the atmosphere and the biosphere; it influences the interaction of the hydrological processes in the earth system over both space and time [4,5]. The SWC is affected by natural and human factors with a certain variability in space and time. The spatiotemporal variation in SWC refers to the obvious difference and diversity of soil moisture characteristics in different regions, at different times, locations, and soil layers [6,7]. Traditionally, SWC can be measured by in-situ observations, remote sensing, and laboratory measurements [3,8]. In recent years, the method of satellites [9,10], proximal neutron [11], and gamma radiation stations [12] have been greatly improved, which promoted the development of soil moisture estimation. SWC is not only subject to spatiotemporal variations related to the diversity of altitude, topography, climate, and human disturbance [13,14] but also affected by variables such as soil properties, precipitation, and the coverage

of vegetation [15,16]. It is widely recognized that the atmospheric-soil-vegetation system is balanced in natural evolutionary processes [17]. The physical process of the water transport system is as follows: After water in the atmosphere falls to the surface in liquid form, some of it penetrates into the soil through the soil pores, and the rest is lost through soil evaporation and evapotranspiration directly from the surface under the effect of the vapor pressure deficit between the surface and the atmosphere. The vegetation interacts closely with hydrometeorological and soil hydrological processes [18,19]. For example, soil moisture and its distribution in desert environments directly affects the number and size of sandy plants [20,21], and also affects the restoration and reconstruction of the degraded ecosystems [22]. Soil desertification always contributes to loss of vegetation coverage and primary productivity, and the lower coverage will exacerbate desertification in turn [23]. Vegetation coverage is a main factor controlling soil erosion and hydrological processes. Generally high vegetation coverage reduces soil erosion and increases surface roughness, and together both prevent or minimize desertification [24]. In the plant-soil system, water supply and water absorption are in dynamic equilibrium, and a stable vegetation cover ensures an increased water holding capacity and SWC, with a beneficial influence on the local microclimate and environmental conditions [25]. Changes in vegetation coverage shift the hydrologic balance and processes of the ecosystem with potential detrimental repercussions at either local or regional scales on the carbon (C) biogeochemical cycle [26,27].

In this paper, we studied two spatially distant sites with high and low grassland coverage to better understand the effects of temporal succession of vegetation degradation in a typical agricultural pastoral ecotone (APE) in Yanchi County, Ningxia. This area is an ecological transitional region characterized by fragility caused by combined effects of changes in land use, climate change, population pressure, economic development and national policies. All these factors have led to landscape fragmentation, desertification expansion, and ecosystem damage [28]. Through the continuous observation of SWC and soil temperature in different areas of grassland—combined with the simultaneous measurement of meteorological and soil variables (i.e., precipitation, temperature, soil particle contents, and organic carbon contents)—the SWC and its spatiotemporal variability were analyzed to understand the pattern and mechanism of the temporal and spatial changes in SWC and to identify the response between precipitation and SWC in the study area. This study provided not only basic data and technical support for further study of the hydrological cycle in the northwest agricultural and pastoral transitional zone but also a theoretical basis for vegetation restoration and tools for combating desertification.

2. Study Area

Yanchi County (106°30′–107°47′ E and 37°04′–38°10′ N) is located in the eastern part of the Ningxia Hui Autonomous Region (NHAR). It is a transitional zone between agricultural and pastoral areas and covers a total area of about 7130 km² (Figure 1) [29]. The south is adjacent to the Loess Plateau and the north borders on the Maowusu Desert. This area has a temperate desert climate with a mean annual air temperature of 8.7 °C, a mean annual wind speed of 2.8 m/s [30], a mean annual precipitation of 280 mm, and a mean annual potential evaporation of 2100 mm [29]. About 60% of the precipitation occurs during the main vegetation growing season of July to September. Vegetation mainly consists of corn and grassland plants such as *Artemisia ordosica*, *Pennisetum flaccidum*, *Glycyrrhiza uralensis*, and *Sophora alopecuroides* [31]. The main soil type is ash-calcite followed by black loess and sandy soil, with loose structure and low fertility [30], making the natural resources of the region diverse and fragile [32].

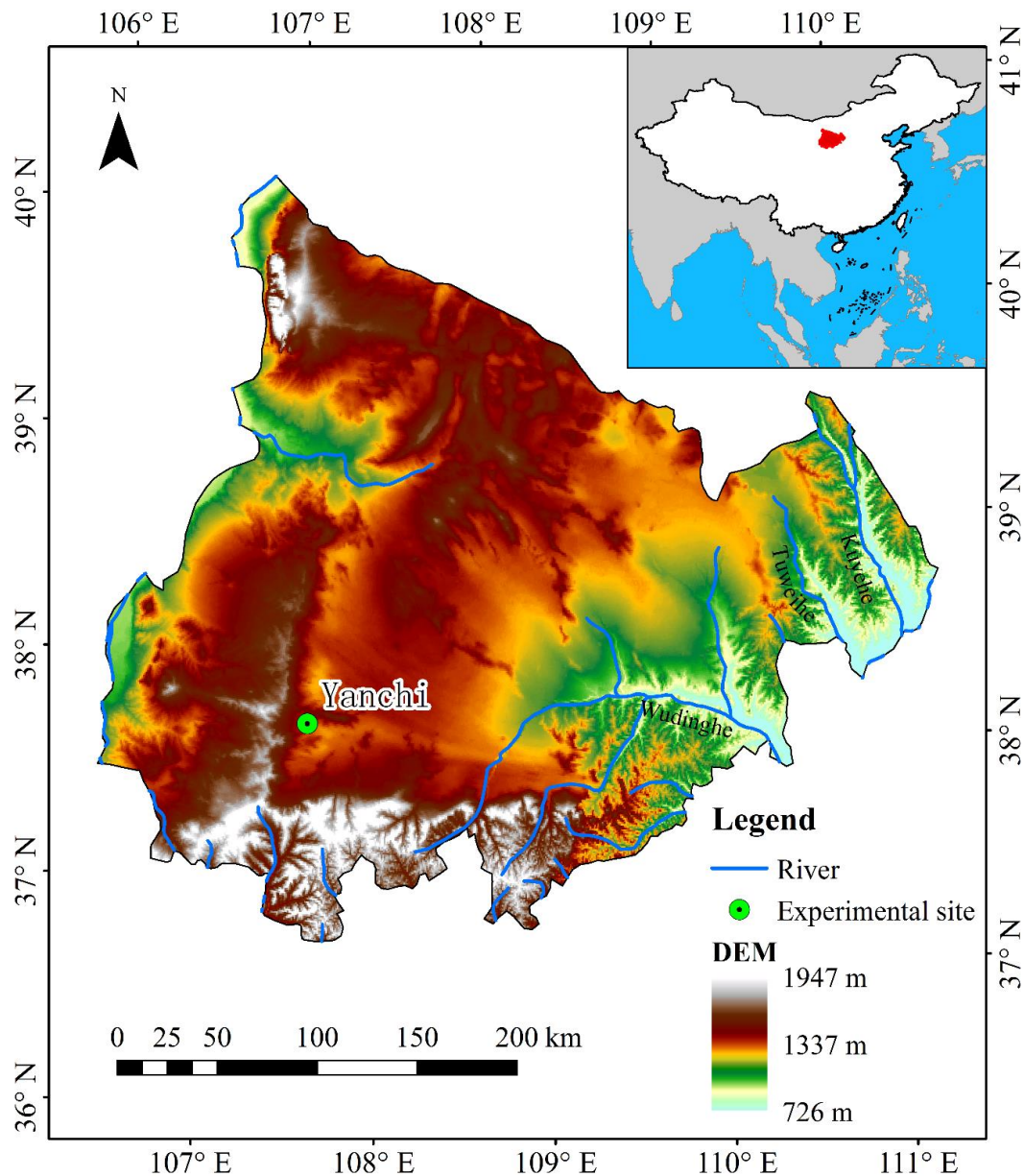


Figure 1. Location of the observational site. The red polygon represents the boundary of the agricultural pastoral ecotone of Northwest China; the green point represents the experimental site; and the blue line represents the river in the study area.

3. Data and Methods

Two typical grassland sites were selected in the study area. The canopy Leaf Area Index (LAI) of the two grasslands was measured by the canopy analyzer (LAI-2000, Li-Cor) in July 2017 [33]. LAI refers to the total area of plant leaf surface per unit earth's surface area, and the larger the LAI, the greater the degree of leaf overlap [34]. Li-Cor's LAI-2000 instrument uses a "fish-eye" optical sensor to measure the transmitted light from five angles above and below canopy and uses the radiation transfer model of vegetation canopy to calculate LAI [35]. We took the mean of the two measured results at each point as the vegetation coverage. The LAI of the high coverage grassland was 0.55 ± 0.1 [m^2/m^2], and that of the low coverage grassland was 0.34 ± 0.1 [m^2/m^2].

A soil profile was manually excavated for each of the two grasslands in July 2017. The two grassland sites were independently analyzed for soil properties for the high and low coverage grassland sites, separately. The soil profiles were divided into five layers (0 ÷ 5 cm, 5 ÷ 10 cm, 10 ÷ 15 cm, 15 ÷ 30 cm,

and 30 ÷ 50 cm) and the soil samples were collected from three different random directions (0.1 kg of soil in each direction) at depths of 2.5, 7.5, 12.5, 22.5, and 40 cm, respectively, in the two soil profiles. Then, the soil samples from the same soil layer of the same profile were uniformly mixed and placed into sealed bags. There were five samples for the high coverage grassland and five samples for the low coverage grassland, both of which correspond to the five depths in the soil profiles. Finally, we brought the mixed sample back to the laboratory to analyze its physical and chemical properties.

A soil moisture monitoring system was installed in each site. The SWC data were collected by the soil moisture monitoring system ECH2O developed by Decagon Corporation [36]. The sensor used 5TE probes, and the data collector was EM50. The 5TE sensor measures the volumetric water content, the temperature of the soil, and electrical conductivity continuously. The 5TE sensor is a capacitance sensor that determines the dielectric permittivity of the medium and using empirical equations to estimate volumetric water content from dielectric permittivity. This sensor minimizes the influence of salinity and texture and is regarded as an accurate sensor in a wide range of soil media [37]. The error of the data was estimated to be within $\pm 3\%$ [38], and this sensor has been used in many studies [3,37,39]. The 5TE probes were inserted horizontally in the soil profiles at depths of 2.5 cm, 7.5 cm, 12.5 cm, 22.5 cm, and 40 cm to measure the SWC and soil temperature at each sampling site. To ensure the quality of the data, the negative values of SWC caused by damaged probes and values less than 2% were removed from data processing. The monitoring period of the in-situ observational system was from 14 September 2016 to 22 April 2019, and data were recorded over 30-minute intervals.

An automatic meteorological station (HoBo U30, hobo) [40] was set up near the two SWC observational systems to make a careful observation of the atmospheric temperature and precipitation. The measurement period was from 14 September 2016 to 22 April 2019, and the measurement frequency was every 10 min.

The particle size of the soil was analyzed by the Mastersizer 2000 particle size analyzer (Malvern Inc, Malvern, England.) [41]. According to the United States Department of Agriculture soil texture classification criteria [42], the soil was divided into clay (particle size $< 2 \mu\text{m}$), silt (particle size $2 \mu\text{m}$ – $50 \mu\text{m}$), and sand (particle size $50 \mu\text{m}$ – $2000 \mu\text{m}$). Soil organic carbon was determined by the carbon analyzer, HT 1300 (Analytik, Jena, Germany) [43].

We calculated the mean values, the standard deviation (SD), coefficient of variation (CV) (i.e. the ratio of standard deviation to mean value), the range, and median to highlight variations that occurred in the SWC at different depths. We also analyzed the dynamic relationship between the SWC and precipitation by the time series. The variation in SWC of the vertical profile was mainly defined by CV. Data analysis and mapping were performed by using Excel 2013 (Microsoft, Redmond, USA), SPSS 22.0 (IBM, New York, USA), and OriginPro 2017 (OriginLab, Northampton, USA).

4. Results and Discussion

4.1. Soil Physical and Chemical Properties

With the decrease of vegetation, the particle size of each soil layer showed a similar change process, that is, the content of clay and silt of low coverage was lower than that of high coverage, and sand content was higher in low coverage grassland (Figure 2). The contents of clay decreased by 71~77% in the first three soil layers (0 ÷ 15 cm), 34% at the fourth layer (15 ÷ 30 cm), and 66% at the fifth layer (30 ÷ 50 cm). The contents of silt decreased by 61~81%, 56%, and 60% at the depths of 0 ÷ 15 cm, 15 ÷ 30 cm, and 30 ÷ 50 cm, respectively. Overall, the contents of clay and silt were significantly depleted in the surface (0 ÷ 15 cm) and deep (30 ÷ 50 cm) layers.

The sand content increased from 79~85% to 94~96% at 0÷15 cm depth, 87% to 94% at the depth of 15 ÷ 30 cm, and 91% to 96% at the depth of 30 ÷ 50 cm. The increased range of sand contents in 0 ÷ 15 cm was larger than those of other depths. It can be seen that when the vegetation was degraded, there was a clear desertification process in the surface soil (0 ÷ 15 cm); the vegetation had an obvious influence on the soil's physical properties. The soil organic carbon content also exhibited significant

changes, decreasing from 0.12~0.18% to 0.06~0.17% across the profiles. The results are consistent with a prior study made by Wang et al., which concluded that vegetation degradation leads to significant degradation of soil physical and chemical properties [44]. Under the different vegetation coverage conditions, sand content within the 30 ÷ 50 cm layer was the highest; clay, silt, and organic carbon contents in this layer were the lowest. As plant roots were mainly distributed at the depth ranging from 0 to 30 cm in the study area, the deep soil of 30 ÷ 50 cm was less affected by vegetation. Thus, it can be seen that the growing process of vegetation was one of the important factors affecting the soil texture and properties. A high rate of vegetation coverage ensures an enrichment in organic matter, which in turn enhances water-retention ability by changing the soil structure and strengthening the adsorption of nutrients into the soil [45], and more water is available in soil for vegetation utilization. In areas with low vegetation coverage the soil does not supply enough water to the plant roots, and the vegetation degradation was further aggravated due to a shortage of nutrients and water.

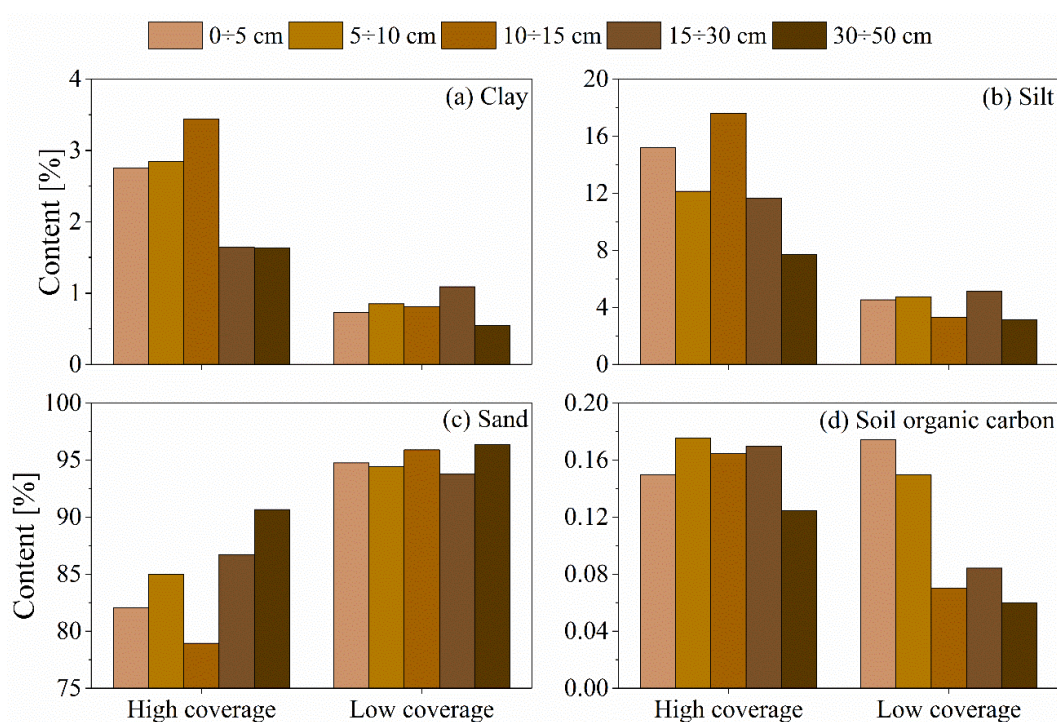


Figure 2. Soil particle content: (a) clay; (b) silt; (c) sand content, and (d) soil organic carbon content in the soil profiles for different grassland coverage.

4.2. Soil Temperature Profiles

Soil temperature plays a crucial role in the soil moisture cycle and thermal balance. Under the different vegetation coverage conditions in the study area, we analyzed the time series of continuous soil temperatures at different depths (Figure 3). The results showed that the fluctuations in soil temperature and air temperature were fundamentally the same. In spring and summer, the surface soil temperature was high, and the deep soil temperature was low. In autumn and winter, the surface soil temperature was low, and the deep soil temperature was high. As the vegetation coverage decreased, the soil temperature of the entire soil profile increased by approximately 8.5 °C. The average annual soil temperature in 0 ÷ 50 cm with high coverage was 10.8 °C, whereas that with low coverage was 19.3 °C. The maximum and minimum daily values of the soil temperature appeared in the 0 ÷ 5 cm soil layer, with a maximum of 35.0 °C in the high coverage grassland and 41.2 °C in the low coverage, and a minimum of −12.3 °C and −9.9 °C in high and low coverage, respectively.

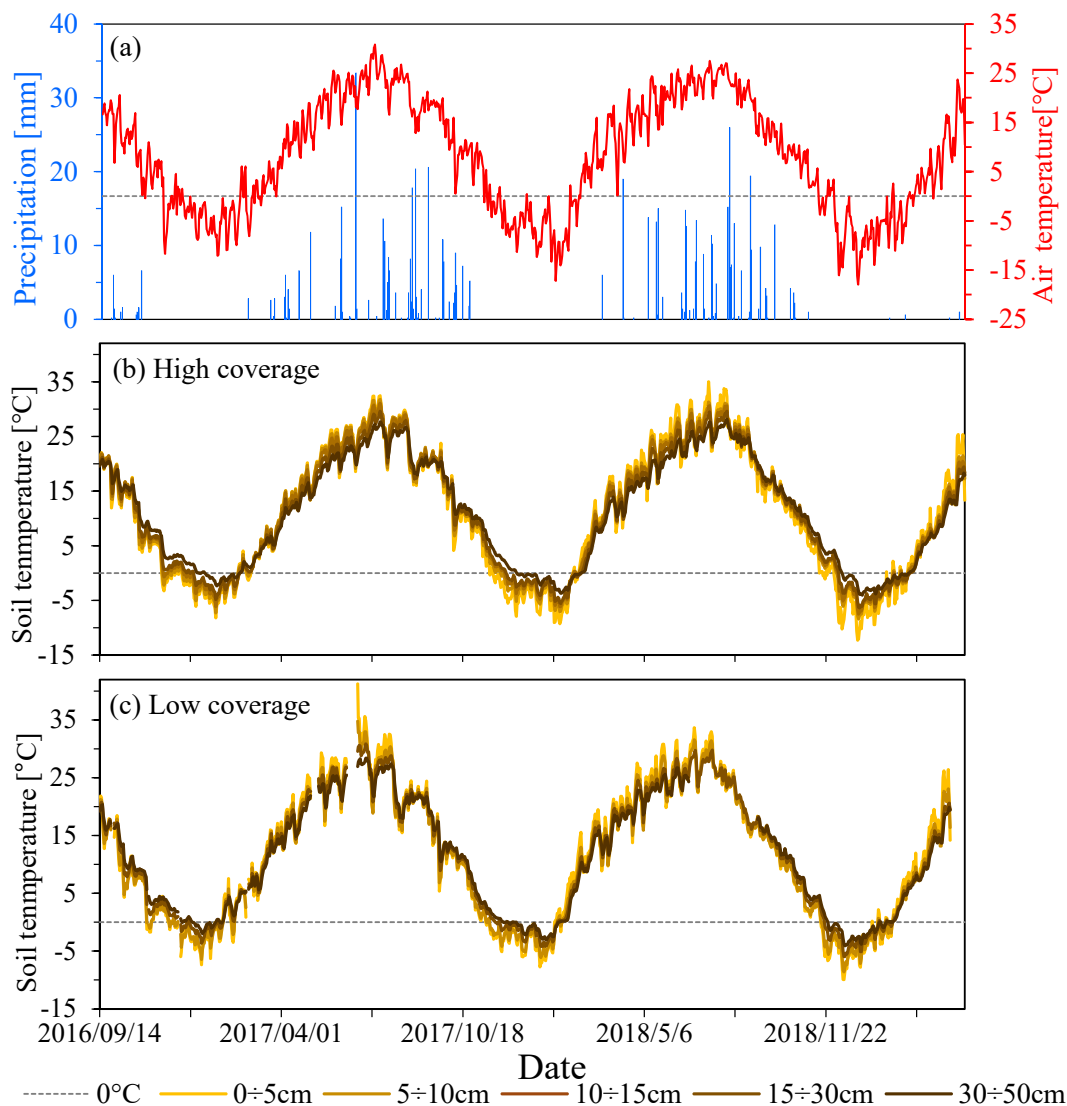


Figure 3. Time series of daily (a) precipitation and air temperature; (b) soil temperature for high coverage, and (c) soil temperature for low coverage from 14 September 2016 to 22 April 2019. Dashed lines represent 0 °C temperature.

Soil temperature was aggregated into daily value over the course of this period. When the soil temperature was continuously less than 0 °C, it was recorded as the frozen date of the soil; when the daily soil temperature was continually higher than 0 °C, it was recorded as the thawed date of the soil [46,47] (Table 1). During 2016/17, 2017/18, and 2018/19, the average of frozen days for the entire soil profile of the high coverage grasslands was 55 days, 83 days, and 78 days, respectively, and 44 days, 69 days, and 73 days for the low coverage, respectively. Generally, the frozen time of all soil profiles in each layer was shortened in the low-coverage grassland compared to that with high coverage. Overall, multi-year average frozen time was shortened by 10 days in low-coverage areas. It indicates that soil temperature responds more strongly to climate warming after vegetation degradation. When the protection of vegetation is lost, the degradation of frozen soil will be aggravated.

In 2017 and 2018, the average increased rate of the soil temperature in soil profiles with high coverage was 0.1958 °C/day and 0.1848 °C/day, respectively; the average decreased values were −0.1887 °C/day and −0.2165 °C/day, respectively. Meanwhile, the average increased rate of the soil temperature with low coverage was 0.2003 °C/day and 0.1962 °C/day; the average decreased values were −0.1913 °C/day and −0.2169 °C/day, respectively. As expected, the increased and decreased rates of the soil temperature with low coverage were both greater than those with high coverage. We

inferred that soil temperature's response to climate change in low coverage was more dramatic and rapid than in high coverage.

Table 1. The soil frozen time for high coverage and low coverage during three frozen periods from 2016 to 2019. The frozen days were counted in five depths, respectively.

Coverage	Year	0 ÷ 5 cm	5 ÷ 10 cm	10 ÷ 15 cm	15 ÷ 30 cm	30 ÷ 50 cm
High	2016–2017	62	61	61	51	39
	2017–2018	95	87	81	83	71
	2018–2019	81	79	77	79	73
Low	2016–2017	50	51	47	47	26
	2017–2018	72	74	73	69	55
	2018–2019	79	78	76	68	64

Vegetation plays a role in slowing down the conversion of heat energy and had a significant effect on the soil temperature. Vegetation absorbs the moisture stored in the soil through the roots, thus reducing soil evaporation and water loss [48]. Degraded vegetation will weaken the cooling effect of plant transpiration on soil temperature, and accelerate the dispersion of water, which will eventually lead to a decrease in SWC. This finding is similar to the study of the influence of vegetation change on soil moisture cycle in an alpine meadow by Wang et al. [49]. Therefore, under vegetation degradation surface soils will be more sensitive to climate change after losing the regulating and protective benefits of vegetation. As a result, soil water-retention capacity, transmission, and migration will be significantly and negatively impacted in degraded soils; ecological environments are rendered increasingly sensitive and fragile.

4.3. Soil Water Content Profiles

Statistical analysis was performed on the in-situ observation of SWC for different depths in each different level of coverage during 14 September 2016 to 22 April 2019 (Table 2). The SWC data in each layer were tested by the Kolmogorov–Smirnov (KS) method, and all of them satisfied the normal distribution. The mean value and median value of the SWC in each soil layer were close to each other. This indicated that the central trend distribution of SWC was not influenced or determined by outlier values and the series of SWC data were reasonable [50]. In general, when the vegetation coverage decreased, the SWC in the same layer was also obviously reduced. The SWC in the 0 ÷ 5 cm and 30 ÷ 50 cm layer was reduced significantly—by more than 39%. SWC losses in other layers ranged from 15% to 25%. The ranges of the CV for high coverage and low coverage were 28~52% and 40~62%, respectively; the CV of the SWC in each layer of low coverage was higher than that in high coverage. It showed that the vegetation degradation exerted a strong influence on the changes in soil moisture, which will reduce the SWC and enhance the degree of variation. The high sand content of low coverage in the deeper soil layer contributed to the poor SWC holding capacity, resulting in a larger variability in the deep SWC.

Observational data indicated that vegetation degradation in the arid regions of Northwest China had a strong influence on the soil's hydrological processes and that plant growth was one of the causes of variability in soil moisture profiles. With the gradual degradation of vegetation, variability in SWC has increased across the soil profiles.

On the seasonal scale, CV at different depths in the summer period was larger than in other seasons (Table 3). Grasslands showed the highest SWC in autumn due to the recharge from precipitation and lower evapotranspiration. The average SWC of the high coverage grassland was 7.4~9.7 [m³/m³] (10⁻²) in spring, 5.7~8.1 [m³/m³] (10⁻²) in summer, 7.7~10.3 [m³/m³] (10⁻²) in autumn, 3.9~6.1 [m³/m³] (10⁻²) in winter; CV ranged from 16% to 52%. The average SWC of the low coverage grassland was 4%~7% in spring, 4.0~7.0 [m³/m³] (10⁻²) in summer, 4.2~7.2 [m³/m³] (10⁻²) in autumn, 2.1~4.4 [m³/m³] (10⁻²) in winter; CV ranged from 18% to 57%.

Table 2. Descriptive statistics of the soil water content (SWC): Mean SWC, standard deviation (SD), coefficient of variation (CV), range, and median from 14 September 2016 to 22 April 2019.

Coverage	Depth [cm]	Mean SWC [m ³ /m ³] (10 ⁻²)	SD [m ³ /m ³] (10 ⁻²)	CV [%]	Range [m ³ /m ³] (10 ⁻²) *	Median [m ³ /m ³] (10 ⁻²)
High	0 ÷ 5	6.9	3.6	52	13.6	6.2
	5 ÷ 10	7.5	2.9	39	11.4	7.2
	10 ÷ 15	7.6	3.0	39	11.3	7.4
	15 ÷ 30	5.9	2.2	37	9.6	5.4
	30 ÷ 50	8.5	2.3	28	9.1	8.1
Low	0 ÷ 5	4.2	2.6	62	11.7	3.2
	5 ÷ 10	5.6	2.4	44	10.2	4.5
	10 ÷ 15	6.5	2.6	40	11.1	5.5
	15 ÷ 30	5.0	2.0	40	9.1	4.2
	30 ÷ 50	5.0	2.1	41	5.3	3.9

* Range: difference between the maximum and the minimum.

Table 3. Descriptive statistics of the average seasonal soil water content (SWC): Mean SWC, standard deviation (SD), coefficient of variation (CV), range, and median from 14 September 2016 to 22 April 2019.

Coverage	Seasons	Depth [cm]	Mean SWC [m ³ /m ³] (10 ⁻²)	SD [m ³ /m ³] (10 ⁻²)	CV [%]	Range [m ³ /m ³] (10 ⁻²)	Median [m ³ /m ³] (10 ⁻²)
High	Spring (Mar–May)	0 ÷ 5	7.4	3.8	52	11.8	8.4
		5 ÷ 10	8.2	2.3	28	8.8	7.7
		10 ÷ 15	8.5	2.1	24	8.6	8.9
		15 ÷ 30	6.6	1.4	21	5.2	5.9
		30 ÷ 50	9.7	1.9	16	5.6	9.4
	Summer (Jun–Aug)	0 ÷ 5	7.6	3.9	52	13.5	6.3
		5 ÷ 10	8.1	3.2	39	10.8	6.8
		10 ÷ 15	7.7	3.3	43	10.6	5.5
		15 ÷ 30	5.7	2.4	42	5.7	4.4
		30 ÷ 50	7.7	1.4	19	7.1	7.3
	Autumn (Sep–Nov)	0 ÷ 5	8.7	2.6	29	11.5	9.2
		5 ÷ 10	9.4	1.7	18	9.6	9.5
		10 ÷ 15	9.7	2.1	21	10.3	9.6
		15 ÷ 30	7.4	2.0	28	7.1	6.5
		30 ÷ 50	10.3	1.8	18	6.1	9.6
	Winter (Dec–Feb)	0 ÷ 5	3.9	1.5	28	6.9	4.1
		5 ÷ 10	4.5	1.4	30	6.1	4.1
		10 ÷ 15	4.6	1.2	26	6.9	4.1
		15 ÷ 30	3.9	0.9	23	5.3	3.5
		30 ÷ 50	6.1	1.5	24	6.9	5.6
Low	Spring (Mar–May)	0 ÷ 5	4.0	2.1	53	9.6	3.2
		5 ÷ 10	5.6	2.3	41	8.0	4.7
		10 ÷ 15	7.0	2.2	32	9.4	6.4
		15 ÷ 30	5.6	1.5	27	5.4	6.1
		30 ÷ 50	5.8	1.9	33	5.8	6.1
	Summer (Jun–Aug)	0 ÷ 5	5.4	3.1	57	11.0	4.2
		5 ÷ 10	6.6	2.8	43	9.3	6.1
		10 ÷ 15	7.2	3.1	43	10.4	5.6
		15 ÷ 30	5.1	2.5	48	8.6	3.8
		30 ÷ 50	4.2	1.4	34	7.6	3.8
	Autumn (Sep–Nov)	0 ÷ 5	6.0	2.3	39	9.7	5.7
		5 ÷ 10	7.1	1.9	27	9.6	7.1

Table 3. Cont.

Coverage	Seasons	Depth [cm]	Mean SWC [m ³ /m ³] (10 ⁻²)	SD [m ³ /m ³] (10 ⁻²)	CV [%]	Range [m ³ /m ³] (10 ⁻²)	Median [m ³ /m ³] (10 ⁻²)
Low	Autumn (Sep–Nov)	10 ÷ 15	7.7	2.3	30	10.2	8.0
		15 ÷ 30	5.9	2.0	35	7.9	6.0
		30 ÷ 50	6.3	2.2	35	7.5	6.0
	Winter (Dec–Feb)	0 ÷ 5	2.1	0.7	36	5.6	2.1
		5 ÷ 10	3.5	0.6	18	5.0	3.4
		10 ÷ 15	4.4	1.0	23	6.0	4.0
		15 ÷ 30	3.5	1.0	28	4.4	3.3
		30 ÷ 50	3.8	1.2	32	5.3	3.4

In spring and autumn, the SWC fluctuations of the first three layers (0 ÷ 15 cm) were similar due to the effect of precipitation, and SWC increased with soil depth (Figure 4). Although the SWC of the first three layers was supplemented by precipitation in summer, their SWC was basically static with no obvious increasing or decreasing trend. It was generally absorbed and transpired by the roots and leaves of the vegetation. In the high coverage grassland, the minimum SWC in each season appeared in the 15 ÷ 30 cm soil layer. Combined with the analysis of soil particle size (Figure 2), the sand content of this layer increased by about 10% compared to the upper layer (10 ÷ 15 cm). The contents of clay and silt were reduced by 52% and 34%, respectively. This meant that the infiltration capacity of the 15 ÷ 30 cm soil layer was better than that of the upper layer, and the water holding capacity was worse. The water percolating from the 10 ÷ 15 cm soil layer was quickly lost, and it was difficult to store at the depth of 15 ÷ 30 cm.

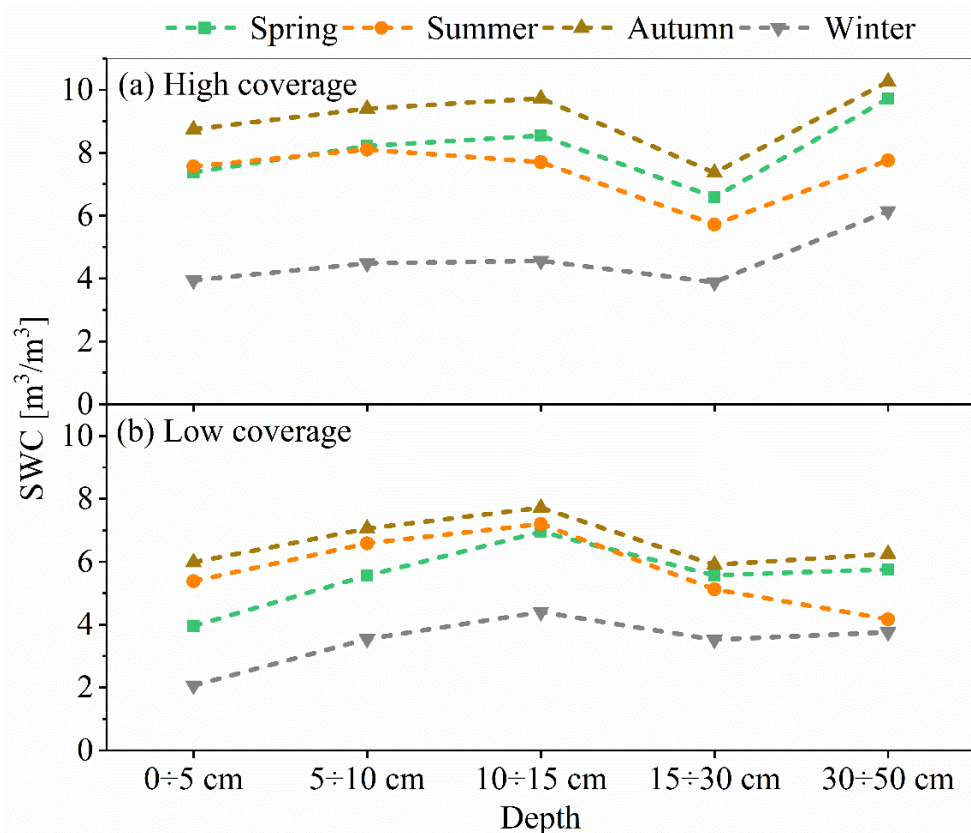


Figure 4. Average seasonal SWC for (a) high coverage and (b) low coverage from 14 September 2016 to 22 April 2019 in different soil layers. Spring is from March to May; summer is from June to Aug; autumn is from Sept to Nov; and winter is from Dec to Feb.

In a study of soil hydrology under different land covers, Tian et al. found that a low coverage grassland led to coarse soil particle size, larger soil porosity, faster infiltration [51], and easier evapotranspiration through the surface layer. Therefore, the soil moisture leakage and evapotranspiration rate were increased and SWC was decreased compared to areas with high coverage in the first three layers of 0–15 cm. Plant roots in the low coverage grassland distributed sparsely. Therefore, they did not show a strong capacity for root water uptake in summer in the first three layers of soil.

4.4. Soil Water Content Response to Precipitation

Atmospheric precipitation is the main source of water supply to soils in the arid regions of Northwest China. The magnitude and process of precipitation have a strong impact on the SWC [3]. SWC response to precipitation in the arid areas was analyzed by comparing the time series of the SWC and the precipitation under different vegetation conditions in the study area of the typical APE during 2017 and 2018 (Figure 5).

Precipitation was relatively low from May to July in 2017. SWC changes in the first three layers (0–15 cm) were basically the same, showing a clear correlation with precipitation. After each precipitation, the direct exchange of water between the 0–15 cm soil layer and the atmosphere occurred. However, SWC was rapidly reduced in the forms of evapotranspiration and infiltration. The reaction of the SWC in the fourth layer (15–30 cm) was slightly delayed with a certain hysteresis. The SWC in the fifth layer (30–50 cm) was not significantly affected by precipitation during this period, although the precipitation on June 1 was significant (33.4 mm). Precipitation did not play a recharging role for the 30–50 cm layer and rainwater was transported by evapotranspiration through the upper soil and the plant root networks. Thus, precipitation could not be accumulated in the deep layer (30–50 cm) during this period.

The precipitation that took place from mid-July to the end of September in 2017 was frequent and heavy. The interaction between rains and SWC in the first three layers (0–15 cm) was rapid. Although root water uptake and the process of evapotranspiration continued naturally, most of the SWC was retained in the soil due to the intensive supply of precipitation, and it was kept in the deep soil (30–50 cm). As a result, low levels of precipitation could not directly recharge the SWC below 30 cm (Figure 5). Only the continuous precipitation that occurred at the end of growing season influenced the deeper SWC. The responsive pattern of the SWC to precipitation in 2018 was similar to that in 2017.

In a study of soil organic matter and water hold capacity in the Tibetan Plateau, Sun et al. found that lower surface soil organic matter content always corresponded with sandy soil and poor water retention [45]. Under the same precipitation conditions, the SWC in the low coverage grassland was rapidly lost in the forms of evapotranspiration due to lower water cycle regulation and interception by plant roots and leaves. Once the ecosystem was degraded and the vegetation coverage was reduced, the energy processes and water cycles between the soil and the atmosphere were altered. Under natural conditions, the self-healing capacity of the ecosystem is fairly limited, and desertification generally occurs in these soils. Compared to the high coverage grassland, the low coverage grassland was more susceptible to changes in soil temperature (Figure 3) and precipitation (Figure 5), which exacerbated the instability and difficulty in restoring grassland ecosystems in the APE arid region of Northwest China.

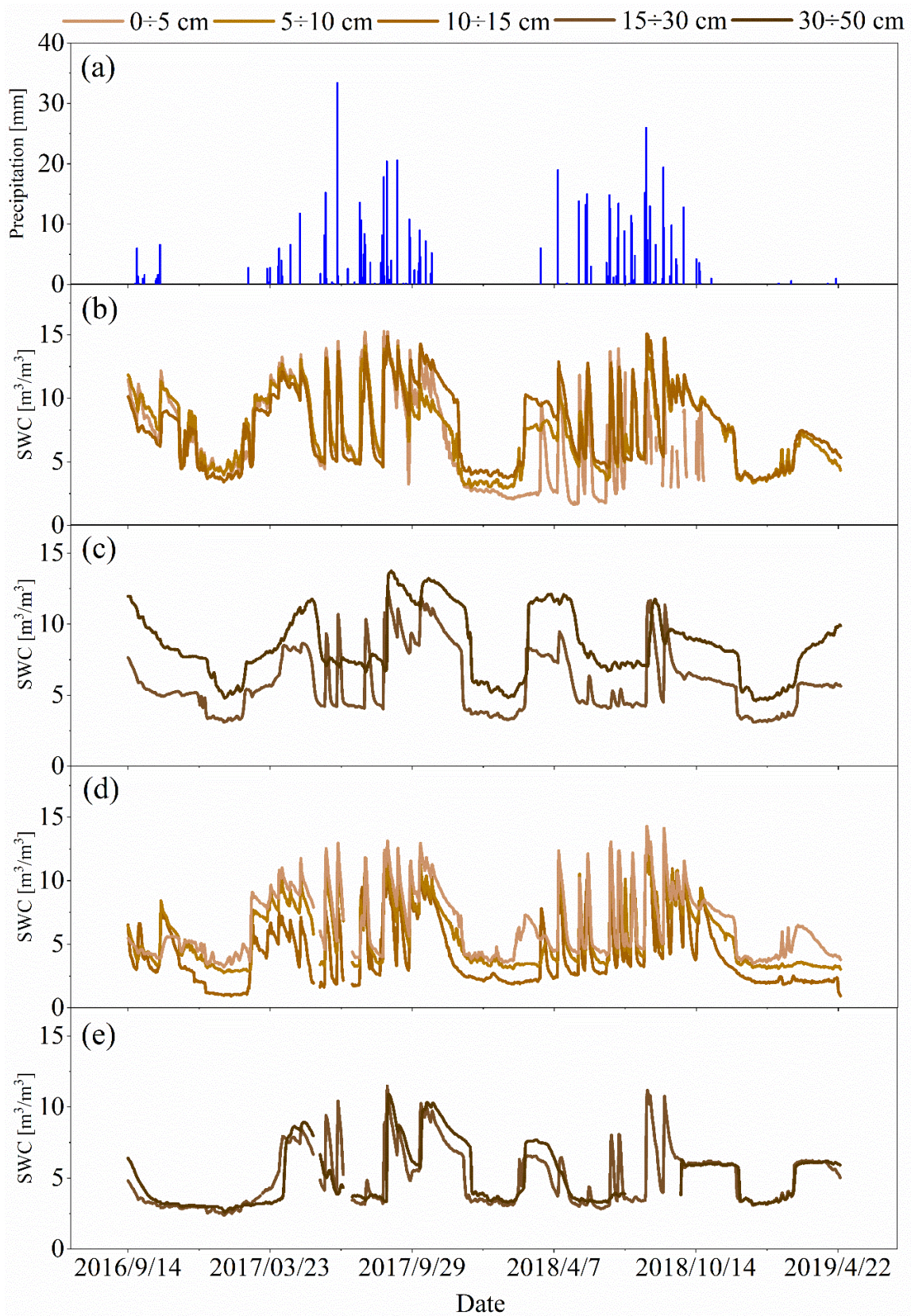


Figure 5. Time series of the (a) precipitation; (b) high coverage grassland SWC for shallow layers (0 ÷ 5 cm, 5 ÷ 10 cm, 10 ÷ 15 cm); (c) high coverage grassland SWC for deep layers (15 ÷ 30 cm, 30 ÷ 50 cm); (d) low coverage grassland SWC for shallow layers, and (e) low coverage grassland SWC for deep layers.

5. Conclusions

Based on the in-situ observations of soil profiles at depths of 0 ÷ 5 cm, 5 ÷ 10 cm, 10 ÷ 15 cm, 15 ÷ 30 cm, and 30 ÷ 50 cm established in Yanchi area of the APE in Northwest China, this study analyzed SWC, soil temperature dynamics, soil particle size content, and organic carbon content in different levels of vegetation coverage. The main conclusions are as follows.

Firstly, degradation of vegetation accelerated the rate of soil desertification. The soil particle size of each layer showed that the sand contents were higher, and the contents of clay and silt particles were lower in the low coverage compared to the high coverage grassland. Meanwhile, the degradation also shortened the multi-year average frozen time by 10 days and increased average annual soil temperature by 8.5 °C during the three-year period in the study. The rates of the soil temperature change with the low coverage grassland were greater than those with high coverage. In addition, the SWC at different depths showed strong spatial and temporal variability. When the vegetation coverage was reduced, the SWC in the same layer declined, especially at depths of 0 ÷ 5 cm and 30 ÷ 50 cm, decreasing by more than 39%. Due to precipitation in summer, the CV of the SWC at different depths was greater than that of other seasons, which also indicated that the existence of plant roots and vegetation growth condition was one of the causes of the variation in the soil moisture profiles. The SWC reaches its maximum in autumn, and only with the abundant precipitation that occurred in the late growing season, the deeper (30 ÷ 50 cm) SWC would be recharged.

Following increasing trends of global warming and climate change, if the vegetation degraded in the arid areas of central Ningxia, then the soil temperature would continue to rise, moisture loss would accelerate, and the SWC would obviously decrease. Unless preventative actions are taken, all of these factors will lead to an irreversible degradation of a fragile ecosystem.

Author Contributions: All the authors contributed to the conception and development of this manuscript. W.Y. and Y.W. carried out the analysis and wrote the paper. C.H. conceived the research. X.T. used the methods for statistical analysis and mapping in the article. Z.H. collected and compiled the data.

Funding: This study was supported by the National Natural Science Foundation of China (41530752; 41877149).

Acknowledgments: Thanks to all the faculty and graduate students for field sampling and monitoring and for their kind help and support. Special thanks to two anonymous reviewers for their constructive comments.

Conflicts of Interest: The authors declare no conflict of interest.

References

1. He, Z.B.; Zhao, W.Z.; Liu, H.; Chang, X.X. The response of soil moisture to rainfall event size in subalpine grassland and meadows in a semi-arid mountain range: A case study in northwestern China's Qilian Mountains. *J. Hydrol.* **2012**, *420*, 183–190. [[CrossRef](#)]
2. Hillel, D. *Environmental Soil Physics*; Academic Press: San Diego, CA, USA, 1998.
3. Tian, J.; Zhang, B.Q.; He, C.S.; Han, Z.B.; Bogena, H.R.; Huisman, J.A. Dynamic response patterns of profile soil moisture wetting events under different land covers in the Mountainous area of the Heihe River Watershed, Northwest China. *Agric. For. Meteorol.* **2019**, *271*, 225–239. [[CrossRef](#)]
4. Pan, Y.X.; Wang, X.P. Factors controlling the spatial variability of surface soil moisture within revegetated-stabilized desert ecosystems of the Tengger Desert, Northern China. *Hydrol. Process.* **2009**, *23*, 1591–1601. [[CrossRef](#)]
5. Albertson, J.D.; Montaldo, N. Temporal dynamics of soil moisture variability: 1. Theoretical basis. *Water Resour. Res.* **2003**, *39*. [[CrossRef](#)]
6. Brocca, L.; Tullo, T.; Melone, F.; Moramarco, T.; Morbidelli, R. Catchment scale soil moisture spatial-temporal variability. *J. Hydrol.* **2012**, *422–423*, 63–75. [[CrossRef](#)]
7. Qiu, Y.; Fu, B.; Wang, J.; Chen, L. Spatial variability of soil moisture content and its relation to environmental indices in a semi-arid gully catchment of the Loess Plateau, China. *J. Arid Environ.* **2001**, *49*, 723–750. [[CrossRef](#)]
8. Tavakol, A.; Rahmani, V.; Quiring, S.M.; Kumar, S.V. Evaluation analysis of NASA SMAP L3 and L4 and SPoRT-LIS soil moisture data in the United States. *Remote Sens. Environ.* **2019**, *229*, 234–246. [[CrossRef](#)]

9. Bauer-Marschallingere, B.; Freeman, V.; Cao, S.; Paulik, C.; Schaufler, S.; Stachl, T.; Modanesi, S.; Massario, C.; Ciabatta, L.; Brocca, L.; et al. Toward Global Soil Moisture Monitoring With Sentinel-1: Harnessing Assets and Overcoming Obstacles. *IEEE Trans. Geosci. Remote* **2019**, *57*, 520–539. [[CrossRef](#)]
10. El Hajj, M.; Baghdadi, N.; Zribi, M.; Bazzi, H. Synergic Use of Sentinel-1 and Sentinel-2 Images for Operational Soil Moisture Mapping at High Spatial Resolution over Agricultural Areas. *Remote Sens.* **2017**, *9*, 1292. [[CrossRef](#)]
11. Andreasen, M.; Jensen, K.H.; Desilets, D.; Franz, T.E.; Zreda, M.; Bogen, H.R.; Looms, M.C. Status and Perspectives on the Cosmic-Ray Neutron Method for Soil Moisture Estimation and Other Environmental Science Applications. *Vadose Zone J.* **2017**, *16*. [[CrossRef](#)]
12. Strati, V.; Albéri, M.; Anconelli, S.; Baldoncini, M.; Bittelli, M.; Bottardi, C.; Chiarelli, E.; Fabbri, B.; Guidi, V.; Raptis, K.G.C.; et al. Modelling Soil Water Content in a Tomato Field: Proximal Gamma Ray Spectroscopy and Soil–Crop System Models. *Agriculture* **2018**, *8*, 60. [[CrossRef](#)]
13. Western, A.W.; Blöschl, G. On the spatial scaling of soil moisture. *J. Hydrol.* **1999**, *217*, 203–224. [[CrossRef](#)]
14. Qiu, Y.; Fu, B.J.; Wang, J.; Zhang, X.L.; Meng, Q.H. Spatiotemporal variation of soil moisture and its relation to environmental factors. *Chin. J. Ecol.* **2007**, *26*, 100–107. [[CrossRef](#)]
15. Penna, D.; Brocca, L.; Borga, M.; Dalla Fontana, G. Soil moisture temporal stability at different depths on two alpine hillslopes during wet and dry periods. *J. Hydrol.* **2013**, *477*, 55–71. [[CrossRef](#)]
16. Li, H.D.; Shen, W.S.; Zou, C.X.; Jiang, J.; Fu, L.N.; She, G.H. Spatio-temporal variability of soil moisture and its effect on vegetation in a desertified aeolian riparian ecotone on the Tibetan Plateau, China. *J. Hydrol.* **2013**, *479*, 215–225. [[CrossRef](#)]
17. Zhang, S.L.; Yang, D.W.; Yang, Y.T.; Piao, S.L.; Yang, H.B.; Lei, H.M.; Fu, B.J. Excessive afforestation and soil drying on China’s Loess Plateau. *J. Geophys. Res. Biogeosci.* **2018**, *123*, 923–935. [[CrossRef](#)]
18. Troch, P.A.; Martinez, G.F.; Pauwels, V.R.N.; Durcik, M.; Sivapalan, M.; Harman, C.; Brooks, P.D.; Gupta, H.; Huxman, T. Climate and vegetation water use efficiency at catchment scales. *Hydrol. Process.* **2009**, *23*, 2409–2414. [[CrossRef](#)]
19. Trancoso, R.; Larsen, J.R.; McAlpine, C.; McVicar, T.R.; Phinn, S. Linking the Budyko framework and the Dunne diagram. *J. Hydrol.* **2016**, *535*, 581–597. [[CrossRef](#)]
20. Nash, M.S.; Wierenga, P.J.; Gutjahr, A. Time-Series analysis of soil-moisture and rainfall along a line transect in arid rangeland. *Soil Sci.* **1991**, *152*, 189–198. [[CrossRef](#)]
21. Pan, Y.X.; Wang, X.P.; Jia, R.L.; Chen, Y.W.; He, M.Z. Spatial variability of surface soil moisture content in a re-vegetated desert area in Shapotou, Northern China. *J. Arid Environ.* **2008**, *72*, 1675–1683. [[CrossRef](#)]
22. Lin, X.R.; Ma, F.Y.; Long, L.Q.; Jia, X.H. Soil water dynamics under sand-fixing vegetation in Shapotou Area. *J. Desert Res.* **2001**, *3*, 3–8.
23. Zhang, Z.H.; Huisingh, D. Combating desertification in China: Monitoring, control, management and revegetation. *J. Clean. Prod.* **2018**, *182*, 765–775. [[CrossRef](#)]
24. Li, F.R.; Zhang, H.; Zhang, T.H.; Shirato, Y. Variations of sand transportation rates in sandy grasslands along a desertification gradient in northern China. *Catena* **2003**, *53*, 255–272. [[CrossRef](#)]
25. McVicar, T.R.; Van Niel, T.G.; Li, L.T.; Wen, Z.M.; Yang, Q.K.; Li, R.; Jiao, F. Parsimoniously modelling perennial vegetation suitability and identifying priority areas to support China’s re-vegetation program in the Loess Plateau: Matching model complexity to data availability. *For. Ecol. Manag.* **2010**, *259*, 1277–1290. [[CrossRef](#)]
26. Zhang, S.L.; Yang, H.B.; Yang, D.W.; Jayawardena, A.W. Quantifying the effect of vegetation change on the regional water balance within the Budyko framework. *Geophys. Res. Lett.* **2016**, *43*, 1140–1148. [[CrossRef](#)]
27. Chen, Y.P.; Wang, K.B.; Lin, Y.S.; Shi, W.Y.; Song, Y.; He, X.H. Balancing green and grain trade. *Nat. Geosci.* **2015**, *8*, 739–741. [[CrossRef](#)]
28. Wei, B.; Xie, Y.; Jia, X.; Wang, X.; He, H.; Xue, X. Land use/land cover change and its impacts on diurnal temperature range over the agricultural pastoral ecotone of Northern China. *Land Degrad. Dev.* **2018**, *29*, 3009–3020. [[CrossRef](#)]
29. Li, Y.; He, T.H.; Qu, X.N. The study on agriculture-animal husbandry industrial adjustment in Yanchi County based on its climate changes. *J. Arid Land Resour. Environ.* **2009**, *13*, 82–86. [[CrossRef](#)]
30. Xu, D.M.; Liu, C.F.; Xie, Y.Z.; Wang, K. Changes of soil properties during sandy desertification for grassland in Yanchi County. *Res. Soil Water Conserv.* **2009**, *16*, 85–88.

31. Li, B. *Study on the Distribution and Hydrological Characteristics of Biological Soil Crusts in Different Desertification Ecosystem Areas*; Beijing Forestry University: Beijing, China, 2015.
32. Cheng, Z.Q.; Zhang, K.B.; Liu, J.; Chang, J.; Wang, X.; Wang, L.L.; Su, P.F. The study on vegetable niche of natural grassland of desertification grassland region in Yanchi County, Ningxia. *Res. Soil Water Conserv.* **2011**, *18*, 36–40.
33. LI-COR Inc. *Plant Canopy Analyzer Operating Manual*; LI-COR Inc.: Lincoln, NE, USA, 1991.
34. Chen, J.M.; Black, T.A. Defining Leaf-Area Index for Non-Flat Leaves. *Plant Cell Environ.* **1992**, *15*, 421–429. [[CrossRef](#)]
35. Garriques, S.; Shabanov, N.V.; Swanson, K.; Morisette, J.T.; Baret, F.; Myneni, R.B. Intercomparison and sensitivity analysis of Leaf Area Index retrievals from LAI-2000, AccuPAR, and digital hemispherical photography over croplands. *Agric. For. Meteorol.* **2008**, *148*, 1193–1209. [[CrossRef](#)]
36. Decagon Devices Inc. *5TE Operator's Manual*; Decagon Devices Inc.: Pullman, WA, USA, 2010.
37. Visconti, F.; de Paz, J.M.; Martinez, D.; Molina, M.J. Laboratory and field assessment of the capacitance sensors Decagon 10HS and 5TE for estimating the water content of irrigated soils. *Agric. Water Manag.* **2014**, *132*, 111–119. [[CrossRef](#)]
38. Bai, X.; Zhang, L.H.; Wang, Y.B.; Tian, J.; He, C.S.; Liu, G.H. Variations of soil moisture under different land use and land cover types in the Qilian Mountain, China. *Res. Soil Water Conserv.* **2017**, *24*, 17–25. [[CrossRef](#)]
39. Zhang, S.Y.; Li, X.Y. Soil moisture and temperature dynamics in typical alpine ecosystems: A continuous multi-depth measurements-based analysis from the Qinghai-Tibet Plateau, China. *Hydrol. Res.* **2018**, *49*, 194–209. [[CrossRef](#)]
40. Carson, T.B.; Marasco, D.E.; Culligan, P.J.; McGillis, W.R. Hydrological performance of extensive green roofs in New York City: Observations and multi-year modeling of three full-scale systems. *Environ. Res. Lett.* **2013**, *8*. [[CrossRef](#)]
41. Callesen, I.; Keck, H.; Andersen, T.J. Particle size distribution in soils and marine sediments by laser diffraction using Malvern Mastersizer 2000-method uncertainty including the effect of hydrogen peroxide pretreatment. *J. Soil Sediment.* **2018**, *18*, 2500–2510. [[CrossRef](#)]
42. Gambill, D.R.; Wall, W.A.; Fulton, A.J.; Howard, H.R. Predicting USCS soil classification from soil property variables using Random Forest. *J. Terramech.* **2016**, *65*, 85–92. [[CrossRef](#)]
43. Boguta, P.; Sokolowska, Z. Statistical relationship between selected physicochemical properties of peaty-muck soils and their fraction of humic acids. *Int. Agrophys.* **2014**, *28*, 269–278. [[CrossRef](#)]
44. Wang, Y.B.; Wang, G.X.; Zhang, C.M.; Long, X.J. Response of soil physicochemical properties to the change of the vegetation ecosystem on the Tibetan Plateau. *J. Glaciol. Geocryol.* **2007**, *6*, 921–927.
45. Sun, Y.; Wang, Y.B.; Sun, Z.; Liu, G.H.; Gao, Z.Y. Impact of soil organic matter on water hold capacity in permafrost active layer in the Tibetan Plateau. *J. Desert Res.* **2017**, *37*, 288–295.
46. Romanovsky, V.E.; Osterkamp, T.E. Thawing of the active layer on the coastal plain of the Alaskan Arctic. *Permafr. Periglac. Process.* **1997**, *8*, 1–22. [[CrossRef](#)]
47. Liu, G.S.; Wang, G.X.; Hu, H.C.; Li, T.B.; Wang, J.F.; Ren, D.X.; Huang, Y.J. Influence of vegetation coverage on water and heat processes of the active layer in permafrost regions of the Tibetan Plateau. *J. Glaciol. Geocryol.* **2009**, *31*, 89–95.
48. Chai, W.; Wang, G.X.; Li, Y.S.; Hu, H.C. Response of soil moisture under different vegetation coverage to precipitation in the headwaters of the Yangtze River. *J. Glaciol. Geocryol.* **2008**, *2*, 329–337.
49. Wang, G.X.; Shen, Y.P.; Qian, J.; Wang, J.D. Study on the influence of vegetation change on soil moisture cycle in alpine meadow. *J. Glaciol. Geocryol.* **2003**, *25*, 653–659.
50. Wang, J.D.; Wang, G.X.; Chen, L. Impact factors to soil moisture of alpine meadow and their spatial heterogeneity. *J. Glaciol. Geocryol.* **2006**, *28*, 428–433.
51. Tian, J.; Zhang, B.Q.; He, C.S.; Yang, L.X. Variability in soil hydraulic conductivity and soil hydrological response under different land covers in the mountainous area of the Heihe River Watershed, Northwest China. *Land Degrad. Dev.* **2017**, *28*, 1437–1449. [[CrossRef](#)]

